Optical Imaging in Biology and Medicine
Master in Photonics & Europhotonics Master Program

Adaptive Optics for Microscopy

Carles Otero Molins
Johannes Rebling
November 27, 2013

Abstract

To achieve optimal, diffraction limited images with the best possible resolution has always been a challenging topic and an important goal in science in general and in biophotonics in particular. Although many new techniques to acquire superesolution images were developed in the last decade, unwanted aberrations often still compromise the resolution and brightness of the images taken with these techniques. Adaptive Optics (AO), a technique that originated in astronomy, is a possible solution to compensate for aberrations in biomedical imaging.

This report presents a review of the numerous applications of AO applied to modern microscopy methods. We review the basic principles of AO, describe how the aberration information is obtained (via direct and indirect sensing) and how AO is applied in the main microscopy techniques (widefield and point scanning techniques). We shown that AO methods have been applied in almost all modern microscopy techniques. However, the increase in resolution and signal quality depends strongly on both the AO and the microscopy technique and great care has to be taken when trying to implement the optimal AO technique.

Contents

1 Introduction

It is well known that optical aberrations degrade the resolution and brightness of images. This results in a reduction of both lateral and axial resolution and a decrease in signal intensity. In general aberrations can be defined as the wavefront distortions with respect to an ideal sphere. These distortions can be cause by imperfections and inhomogeneities in any part of the optical system. In microscopy, aberrations may arise from the microscope itself or the specimen under study [9]. Aberrations always limit the final image quality and can vary from one specimen to another. In this case they can not be corrected by a optimized optical design which makes dynamic correction necessary.

It is of little surprise that scientists have been trying to overcome this problem for many years, an effort that resulted in what nowadays is called Adaptive Optics (AO). The first proposal of the use of AO technology was suggested in the year 1953 in the context of astronomical optics for the compensation of the aberrating effects of the atmosphere [5].

The main idea of AO is the modulation of an incoming wavefront in such a way that we can record an image without aberrations. It is based upon the principle of phase conjugation: the correction element introduces an equal but opposite phase aberration to that present in the optical system. In order to do that, we need to be able to measure these distortions reliably. The most direct way is to use a wavefront sensor, such as the Shack-Hartmann [37, 30] or Curvature Sensors [33]. Also, interferometric techniques have been used to measure aberrations [40]. Furthermore, there are indirect or sensorless methods in which aberrations are determined using and optimization algorithm and do not employ a direct wavefront sensing [8]. A control system then processes the aberration information and uses it to control and adaptive correction element. The adaptive element is needed to modulate and correct the incoming wavefronts before the light reaches the imaging detector. This task is usually performed by a deformable mirror or a liquid crystal spatial light modulator (LC-SLM).

Although Adaptive Optics systems have been sucessfully introduced in applications such as astronomy, laser beam shaping, optical communications, data storage and ophthalmology [10], it is not trivially applied to microscopy. One particularly difficult problem in AO microscopy is how the aberration information is obtained in each of the different microscopy techniques, since direkt sensing can usually not be easily implemented as it is the case in astronomy.

Optical microscope techniques can be divided in two main groups: the widefield techniques and the point scanning techniques. Examples of the first group are the conventional transmission microscopy, the structured illumination microscopy and the fluorescence microscopy. Some point scanning techniques are the confocal microscopy, Stimulated Emission Depletion (STED) or the non-linear microscopy such as Two-Photon Excitation Fluorescence (TPEF), Second Harmonic Generation (SHG) microscopy, Third Harmonic Generation (THG) microscopy and Coherent anti-Stokes Raman (CARS).

In order to explain how adaptive optics and microscopy are linked together, we will start explaining the basis of adaptive optics. This includes a brief review of the concept of aberrations and how they are most commonly characterized. After that, we will explain in more detail the main methods for wavefront sensing, the main aberration corrector devices and some control strategies. Furthermore, we will show some applications of the AO in different widefield and point scanning microscopy techniques. The last part will be a short explanation of future prospects and conclusions.

2 Aberration Measurement and Correction

In practice, no optical system can be totally free from aberrations. That means that all the rays originating from the same object point and going through an optical system will not converge into the same point at the image plane. In other words, the wavefront is distorted with respect to an ideal one when passing through a real system. Thus, we can define the wavefront aberration function as the optical path difference between the aberrated (real) wavefront and the reference (perfect) wavefront. These aberrations can be introduced both upon reflection from a non-planar surface and by passing through an inhomogeneous media as shwon in Fig. 1.

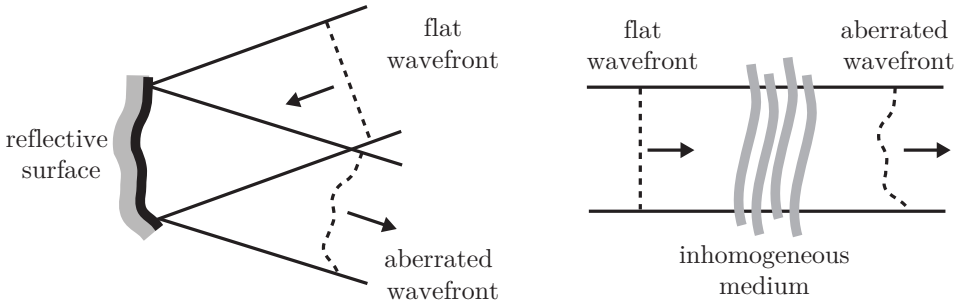

(a) Reflection. (b) Transmission.

Figure 1: Wavefront aberrations due to (a) reflection from a non planar surface and (b) caused by propagation through a non-uniform refractive index distribution [9].

In biological microscopy, the two potential sources of aberrations are the optics and the specimen under study. Regarding the optics, one important parameter is the Numerical Aperture (NA) since aberrations become more significant for those microscopes employing higher NA objectives. Aberrations can also be produced by the difference of refractive index between the microscope coverslip and the specimen mounting medium. Regarding the specimen, aberrations are caused by the variations in refractive index due to the three-dimensional nature of cells and tissue structures. These sample induced aberrations generally become dominant when the image focus lies deep within the sample, since light hast to pass a large distant trough an inhomogeneous medium [9].

There are different ways to characterize the aberrations mathematically. In systems with circular symmetry (circular apertures) it is very common to use the Zernike polynomials because they form a complete, orthogonal set of functions defined over a unit circle [42]:

$$W(\rho,\phi) = \sum_{n}^{k} \sum_{m=-n}^{m=n} {c_n}^m {Z_n}^m(\rho,\phi), \tag{2.1}$$

where $W(\rho,\phi)$ is the wavefront aberration function in polar coordinates at the exit pupil, c_n^m are the Zernike coefficients and $Z_n^m(\rho,\phi)$ are the Zernike modes (or polynomials). As we can see in the equation, the wavefront aberration function is a linear combination of polynomials. Therefore, the more polynomials (i.e. modes, $Z_n^m(\rho,\phi)$) we can measure, the better characterization of the $W(\rho,\phi)$ function we have. Representing aberrations in this way can simplify the design, control and characterization of the Adaptive Optics system.

Although it is known where the aberrations come from, it is not always easy to measure them and implement the measure inside the optical system. There are different classifications of wavefront sensing in the bibliography [38]. Here we will use the one employed by *Martin J. Booth* [9] and we will explain the most common methods of wavefront sensing applied to microscopy.

2.1 Direct Wavefront Sensing

Direct Wavefront Sensing is based on a direct measure of the phase gradient or the wavefront slope, it is considered as an aperture-plane sensing. Within this group there are several techniques such as interferometric, although in general the most used is the Shack-Hartmann.

This last technique is based on a two-dimensional array of a few lenslets -a matrix of microlens-, all with the same diameter and the same focal length, that allows us to measure the wavefront's slope at the exit of the optical system. In other words, it allows us to reconstruct the wavefront aberration function from the local slope's changes of an aberrated wavefront in relation with a reference wavefront. That is achieved measuring the displacements $(\Delta x, \Delta y)$ from each image given by each microlent (Fig. 2).

We start from an aberrated beam going through the matrix of microlens before it is detected in a recorder device. The beam is then spatially sampled into many individual beams (one for each microlens) by the lenslet matrix and forms multiple spots in the focal plane of the lenslets. Finally, the

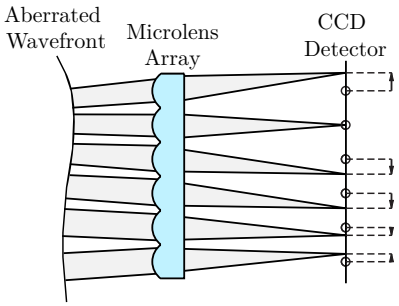

Figure 2: Two-dimensional section of Shack-Hartmann matrix of microlens. When an incoming wavefront goes through the matrix is divided in multiple beams. In the focal plane of the matrix we have multiple spots. If the wavefront is not aberrated, each spot will be placed along the axis of each microlens. If it is aberrated, it will be displaced with respect to this axis. Image after [25].

recorder device -that is placed at the focal plane of the matrix- registers multiple spots. This device is usually a CCD camera. The typical lenslet diameters range from about 100 to 600 mm and the typical focal lengths range from a few millimeters to about 30 mm [31].

We must note that direct sensing needs a well defined wavefront in the pupil of the system or in other words, a point-like emitter. An this situation might not happen in biological microscopes where we are studying three-dimensional specimens, because the light emitted by the specimen may come not only from the focal point. This fact brings us to a couple of problematic situations. The first one is the superposition of wavefronts in the pupil which its effects will depend on the coherence of the emitted light. If it is coherent we will have interference in the pupil, thus we will have ambiguous sensor readings and this kind of sensing will not be suitable for aberration correction. In this sense, if in the focal region the specimen behaves as a point-like scatterer (it will emit incoherent light) the sensor will be able to measure the aberrations produced in the emission path, which in principle they should be the same as in the illumination path. But, if our specimen acts as a planar mirror-like in the focal region, the sensor will just be able to measure twice the even components of the aberrations produced in the illumination path (or emission path), that is because the "'mirror behavior"' will spatially invert the aberrations in the illumination path (Fig. 3). Let us analyze it in detail. We know that the measured aberration ($W(\rho,\phi)$) is the sum of the illumination an emission path aberrations. Also we can denote the measured aberration as the sum of its even and odd components. All together become,

$$W(\rho,\phi) = W(\rho,\phi)_i{}^{even} + W(\rho,\phi)_i{}^{odd} + W(\rho,\phi)_e{}^{even} + W(\rho,\phi)_e{}^{odd}, \tag{2.2}$$

Due to the spatial inversion we know that $W(\rho,\phi)_i^{even} = W(\rho,\phi)_e^{even}$ and $W(\rho,\phi)_e^{odd} = -W(\rho,\phi)_e^{odd}$, therefore the measured aberration can be simplified as,

$$W(\rho,\phi) = 2W(\rho,\phi)_e \tag{2.3}$$

We have shown that in planar mirror-like structures we lose information about aberrations. Thus, in this cases it is not a good option to implement a direct sensing. Regarding microscopy techniques, we must note here that fluorescence emission is an incoherent process, but the non-linear processes generate a coherent signal.

The other problematic situation that we can have in direct sensing due to three-dimensional nature of the specimen is that our sensor might detect more intensity signal from the light scattered out-of-focus than the scattered in the focal region. In order to overcome this problem it can be used a spatial filter between objective and sensor. This filter performs in a similar way than the pinhole used in confocal microscopy. Also it is possible to use coherence gating to exclude out-of-focus light instead of the spatial filter, although it is a more complex method. We must recall here that the light emitted in the

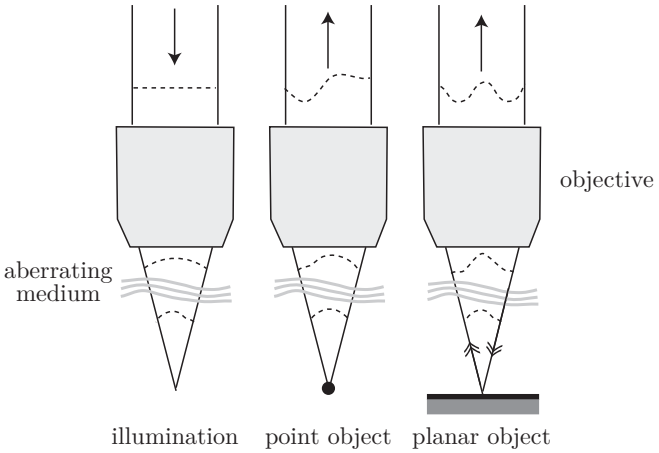

Figure 3: Representation of the two effects due to the specimen structure on wavefront measurements. The left figure shows how the wavefront is aberrated in the illumination path. In the center it is shown a point-like scatterer. Only the emission path is measured. In the right figure it is shown a planar reflector. The illumination wavefront is spatially inverted on reflection before acquiring further aberration in the detection path. Image after [9].

non-linear processes is confined mostly in the focal region.

2.2 Indirect Wavefront Sensing

While direct wavefront sensing techniques are widely applied in Astronomy, they are less common in microscopy techniques. This for several reasons. It is not as easy to create a guiding start like point source in a biological specimen. If there are not features in the specimen that occur there naturally and which resemble a point source, one has to be implemented manually which might alter the function of the specimen or might even be toxic to the sample. Modern microscopes are also highly complex and optimized, which makes it difficult to insert a relatively large wavefront sensor. For samples with weak signal strength, it is also desirable to collect as many photons as possible for the imaging process. Splitting the beam and using a part of the light emitted from the sample for direct wavefront sensing might hence decrease the signal strength too much.

Indirect techniques do not measure the wavefront directly but instead optimize some merit function that depends on the optical system. Indirect methods are used more often in industrial and medical applications. They usually require very little additional hardware. Once the technique is optimized for a specific problem, indirect schemes are easier to implement in practice and are more prone to errors due to the lack of additional hardware (a single deformable mirror might be sufficient to implement adaptive optics in an existing microscope). These techniques can be divided as stochastic or image-based ones. Within the stochastic indirect sensing techniques there are several algorithms. One of the most popular is the genetic algorithms. In this algorithms we start from a random set and we apply an iterative selection of the best solutions. These genetic algorithms do not require any preliminary information about the system but they require more time. The basis of genetic algorithms is that they try to overcome a problem by simulating the evolution process. They start from a population of possible solutions and save some of the strongest elements that are those selected to survive, which means that are able to be reproduced and give the next generations. The probability in which the inferior solutions survive and reproduce is smaller. In general terms, the basic steps for this algorithms are: 1)Chose a random set of possible solutions, 2)Selection function, 3)Reproduce the function in order to create the new generations, 4)Evaluate the possible solutions, 5)Repeat from step 2. For the sake of brevity, we recommend these references for a further reading [39],[1] and [18]. Now we are going to proceed to explain a general description of the image-based techniques.

For these techniques, the optimization of an image quality metric is mainly a mathematical rather than a technical problem. The aberration correction is performed through an iterative optimization

of an image quality metric based. The metric is usually based on spatial frequencies [13] or image intensity [17]. Such optimization is either implemented empirically or by using an appropriate mathematical model. In many practical systems aberrations can be accurately represented by a small number of modes of an orthogonal basis, such as Zernike polynomials. A sequence of images is acquired, each with a different aberration applied and the correction aberration is estimated from the information in this images. This process is repeated until the image quality is considered acceptable. The number of measurements needed to obtain an acceptable image depends strongly upon the optimization algorithm and parameters used, the mathematical representation of the aberration, and the object structure. For the earliest and most generic algorithms the number of measurements per aberration mode increases quadratically or exponentially with N, the number of corrected aberration modes [7]. The so called direct maximization method (as described in Section 3.1.1) is significantly more efficient, requiring only $N+1$ measurements for N mode. With this technique, Lukosz polynomials [23] are used to classify the aberrations. The effects of different modes can then be separated and the optimization of each mode becomes independent and hence more efficient.

An effective model-based adaptive optics scheme should also be independent of the imaged object and should permit the separation of aberration and object influences on the measurements. This separation is also possible through the appropriate choice of optimization metric and aberration representation [13]. The interested reader will find more information on the mathematical background in reference [32, 7, 23, 13].

2.3 Aberration Correction

The wavefront correctors are the essential device of an adaptive optics system. Their aim is to provide a certain phase profile of the incident wavefront by changing the physical length over which the wavefront propagates or the refractive index of the medium through which the wavefront passes. They are based on mirror technology (Fig. 4) or on liquid crystal technology. The first ones change the phase by adjusting their surface shape (i.e., change their physical length while keeping the refractive index constant) and the second ones keep the physical length constant and rely on localized changes in refractive index. The mirror-based correctors are wavelength and polarization independent and can be reconfigured at rates of a few kilohertz [9]. They can have a continuous surface (i.e., discrete actuator, bimorph or membrane mirrors) or segmented surface (i.e. piston-only or piston/tilt mirrors). Unlike continuous mirrors, the segmented mirrors have gaps between the segments that reduce the efficiency and quality of the correction, although they can achieve much better wavefront fitting.

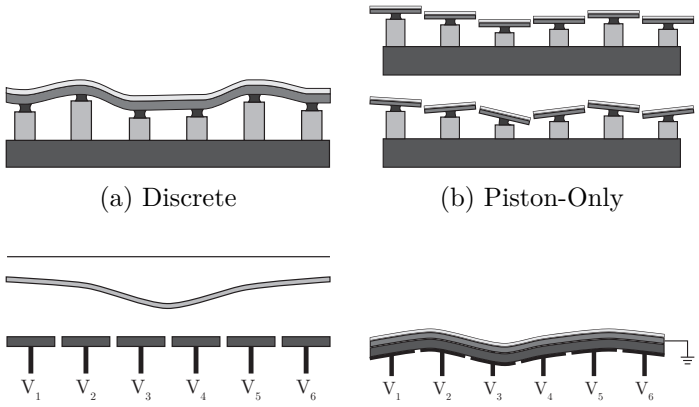

(a) Discrete (b) Piston-Only

(c) Membrane (d) Bimorph

Figure 4: The four main mirror correctors. (a) Discrete actuator deformable mirrors consist of a continuous, reflective surface and an array of actuators, each capable of producing a local deformation in the surface. (b) Piston-only segmented correctors consist of an array of small planar mirrors whose axial motion (piston) is independently controlled. Piston/tip/tilt-segmented correctors add independent tip and tilt motion to the piston-only correctors. (c) Membrane mirrors and (d) Bimorph mirrors. Image after [31].

Regarding the liquid crystal-based mirrors, they change the refractive index electronically or optically, are wavelength and polarization dependent and can reach velocities of just a few tens of hertz. The nematic liquid crystal is the most common for AO applications. In general, they are much cheaper than the mirror-based correctors, are capable of producing more complex phase patterns but they have lower light efficiency.

In AO microscopes the first choice in most cases is the deformable mirror because of their high detection efficiency. Besides, they are better suited for fluorescence techniques due to their polarization independent behavior. However, in particular cases, LC-SLM can be enough if aberration correction is only needed in the illumination path.

3 Adaptive Optics Methods applied in Microscopy

Adaptive optics techniques have found their way into almost all kinds of modern, high resolution microscopy techniques. These microscopes have been combined with direct wavefront sensing and sensorless AO, using deformable mirrors or spatial light modulators for aberration compensation (all of which has been described in Section 2. This includes standard widefield microscopes as well as highly sophisticated and specialized point scanning methods such as Coherent Antistokes Raman Spectroscopy (CARS) and Stimulated Emission Depletion (STED) techniques. It has to be noted however, that some of these methods are themselves only a few years old. Therefor, they are still being optimized and so are the AOM techniques. It is therefore an interesting field of research with new ideas being implemented every year.
AO was first used in confocal and two-photon fluorescence microscopy, both of which are commonly used in biomedical applications. These microscopes suffer from a significant drop in signal and resolution as the focus is moved deeper into the specimen, which is caused by aberrations [35].

AOM is also used for imaging of live specimens. Due to an increased excitation signal and improved light collection from the specimen, acquisition times can be reduced and contrast can be enhanced. Techniques that without AO are to slow for live imaging might now be usable, opening up completely new fields of research. Another advantage of AO lies in the microscopy design. Using AO methods, can help the designer to relax the aberration tolerance. This permits a significant reduction in the complexity of the optical system while maintaining diffraction limited operation.

This section will describe, using state of the art examples, how AO is implemented in both widefield and point scanning systems.

3.1 Widefield Microscopy

As mentioned above, AO techniques are being applied in widefield microscopy. In conventional microscopes, widefield illumination is provided using back light illumination or in the case of reflection or fluorescence modes, via the objective lens. The image quality depends only on the aberrations induced in the detection path and is independent of the aberrations of the illumination path. Aberration correction is therefore only necessary in the detection path and a single pass adaptive optics system will suffice [24]. Hence, the goal of AO for widefield microscopy is to restore the best possible imaging and to correct for aberrations induced both by an imperfect imaging system as well as by the imaged specimen. The latter becomes more important for thick biological samples where the light has to travel a larger distance through a medium with an inhomogeneous refractive index.

Many other highly specialized widefield microscopy techniques have been developed and for most of those, AO schemes for aberration correction and resolution optimization have been presented. Two widefield microscopye techniques will be presented in this section. First the implementation of AO in a standard transmission microscope (Section 3.1.1) using a sensorless wavefront sensing scheme is explained. How the theoretical background of this technique can be applied to more sophisticated microscopy schemes is then shown on the example of structured light illumination (Section 3.1.2), a specialized wide field technique.

Not covered by this report is the application of AO using a direct wavefront sensing scheme as presented by *Azucena et al.* in 2011 using a Shack–Hartmann wavefront sensor, a fluorescent reference

source, and a deformable mirror [4].

For fluorescence microscopy, the aberration caused by an refractive index mismatch between sample, cover plate and immersion medium can by calculated theoretically and is then corrected [22] or the aberration is measured using a guide-start technique [3] as described in Section 2. Since the techniques applied in fluorescence microscopy are very similar to the ones presented for transmission microscopes, they will not be explicitly covered here. AO is also applicable in multifocal multiphoton microscopy [6, 12].

3.1.1 Transmission Microscope

To implement adaptive optics with standard (incoherent) transmission microscopes, *Debarre et al.* [13] implement an indirect, sensorless and image-based adaptive optics scheme, as shown in Fig. 5. As described earlier in Section 2.2, image-based techniques do not require an additional wavefront sensor but retrieve the correction data directly form the recorded images. As with all indirect sensing schemes, the difficulty is to find a good metric for image quality, which allows to determine the appropriate correction parameters.

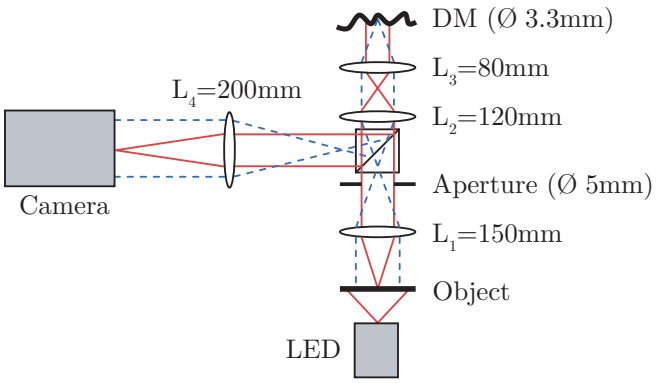

Figure 5: Schematic diagram of the experimental setup, showing a simple microscope complemented with a deformable mirror for aberration correction. Image after [13].

The presented method uses low spatial frequency content of the image as the optimization metric. The aberration is represented in terms of so called Lukosz modes. Like Zernike polynomials, the Lukosz functions are each expressed as the product of a radial polynomial and an azimuthal function. The presented technique is based on modeling the effects of aberrations on the imaging of low spatial frequencies, which Lukosz modes are are found to be ideal for.
By modeling the aberration $\Phi(r)$ as a series of N Lukosz modes $L_i(r, \phi)$ with coefficients a_i [23]:

$$\Phi(r) = \sum_{i=4}^{N+3} a_i L_i(r, \phi), \tag{3.1}$$

they develop the optimization metric g as the sum of a range of low frequencies. It is related to the coefficients of the aberration expansion, a_i by the Lorentzian function [13]

$$g(a_i) \approx \frac{1}{q_0 + q_1 \sum_{i=4}^{N+3} a_i^2} \tag{3.2}$$

where the piston, tip and tilt modes ($i = 1, 2, 3$ respectively) have been omitted and q_0 and q_1 are both positive quantities in the frequency range of interest. The aberration correction process is then performed as the maximization of $g(a_i)$. Because of this particular aberration expansion and optimization metric, the function $g(a_i)$ shows a paraboloidal maximum that permits the use of simple maximization algorithms. Furthermore, it is shown that the optimization can be performed as a sequence of independent maximizations for each aberration coefficient.

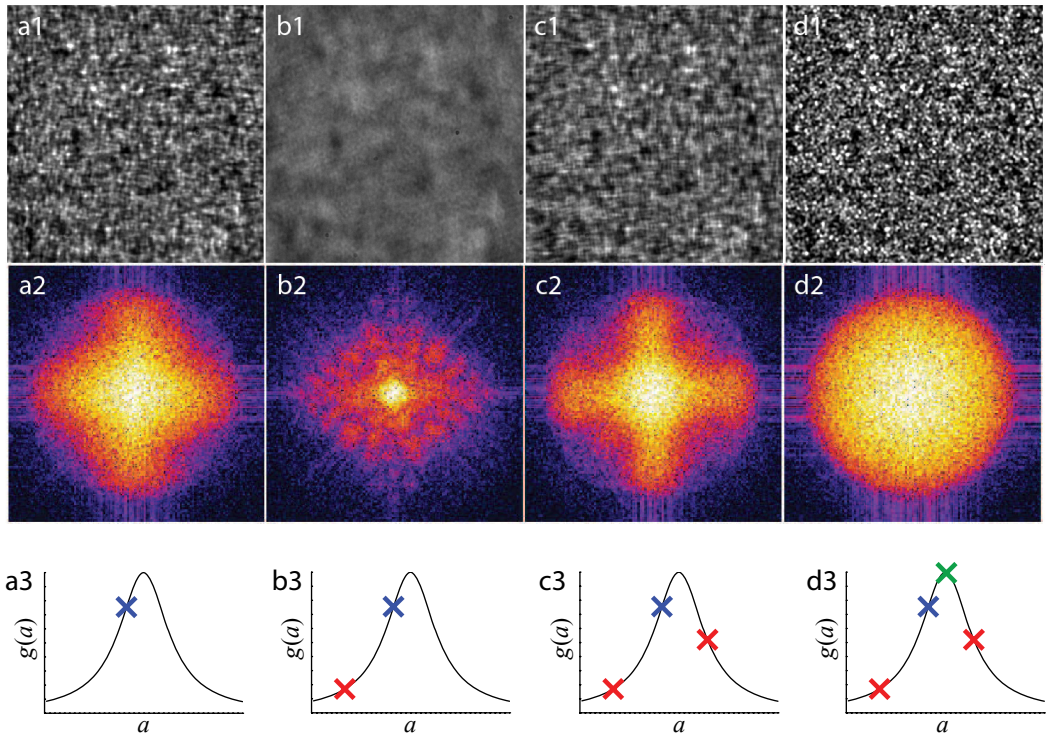

Figure 6: Correction of a single Lukosz aberration mode (astigmatism, i = 5) for a scatterer specimen and using low spatial frequencies. The first row shows the raw images of the specimen and the second row contains the corresponding spectral densities. The third row illustrates schematically the sampling of the Lorentzian curve used in the optimization calculation. (a1-a3) correspond to an arbitrary initial aberration of magnitude, (b1-b3) have an additional negative bias while (c1-c3) have an additional positive bias of equal magnitude. (d1- d3) show the corrected image calculated with the parabolic minimizationn. Image after [13].

The correction process is shown in Figure 6 for the correction of a single Lukosz mode using a scatterer specimen. Using the deformable mirror (DM), an initial aberration a_i is applied and an image is recorded. The Fourier transform and spectral density of the image are then calculated and the appropriate range of frequency components are summed, giving the metric measurements g_0. The same procedure is repeated with both negative and positive aberrations (i.e. stronger and weaker aberrations), resulting in the metric measurements g_- and g_+. Due to the paraboilc maximum of Eq. (3.2), the value of a_i that minimizes g can be calculated from as little as three measurements of $g(a_i)$. The optimum correction aberration can then estimated by parabolic minimization as [32]:

$$a_{\text{corr}} = \frac{b(g_+ - g_-)}{2g_+ - 4g_0 + 2g_-} \tag{3.3}$$

and is then applied to the DM. To correct multiple modes, each modal coefficient is measured in the same manner before the full correction aberration containing all modes is applied. While this technique is based only on low spatial frequencies, it is shown that both low and high frequency components can be effectively corrected. In all the cases investigated, a Strehl ratio greater than 0.8, close to the diffraction limit, was obtained. This indicates that, when aberration statistics are unknown, choosing small spatial frequencies for an initial correction is a reasonable strategy. If further correction is required,they can be performed using a larger range of frequencies. *Debarre et al.* conclude that this correction scheme is largely independent of the object structure and propose that this approach also to be valid for coherent or partially coherent systems.

While the scheme presented above has the advantages of only needing a deformable mirror and no extra wavefront sensor, it also requires a lot of time to quire the necessary $2N + 1$ images. It is also

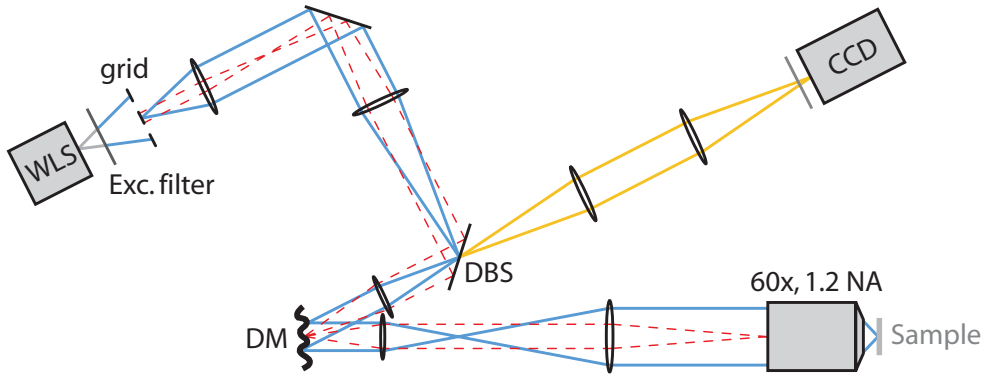

Figure 7: Experimental setup for structured illumination microscopy with aberration correction. WLS - white light source, DM - deformable mirror, DBS - dichroic beamsplitter. The blue rays mark the illumination path; the detection path is shown in yellow. Image after [14] .

inflexible, since the model used for the optimization is depending on both the imaging system and the sample. Another approach is to use a direct wavefront sensing scheme, as presented by *Azucena et al.* in 2010 [3]. Until their publication, most AOM system only measured the wavefront indirectly due to the added complexity and the lack of natural point-source references such as the "guide-stars" used in astronomy and vision science. The authors overcome the latter problem by introducing a suitable fluorescent point source reference beacon as an artificial guide-star into the sample.

Fluorescent microspheres can be engineered in a large variety of colors and are often used in biology. The microspheres can be manufactured with coatings to preserve them in different conditions and to target different biological tissues, organelles, cell walls, or other biological structures [14]. There are also various ways to introduce them into the sample such as negative pressure injection, pressure injection, matrotrophycally and diffusion. *Azucena et al.* in particular inject small fluorescent microspheres into Drosophila embryos where they are diffraction limited when imaged by the Shack- Hartmann wavefront sensor. Hence they can be used as a point source, enabling effective wavefront sensing. After the microspheres were injected sucessfully, the applied wavefront sensing in correction technique is very similar to the one described used by *Aviles-Espinosa et al.* [2] and described in Section 3.2.2. We will therefor not further elaborate on this technique here. The final data analysis of *Azucena et al.* demonstrated that their approach can improve the Strehl ratio by 2 times on average and as high as 10 times when imaging through 100 µm of tissue.

3.1.2 Structured Illumination Microscopy

It is often desired for biological samples to produce clear images of focal planes deep within a thick sample (i.e. optical sectioning) and common techniques include point-scanning techniques such as confocal or multiphoton techniques which are described in Section 3.2.

Widefield techniques such as Structured Illumination (SI) microscopy can also provide optical sectioning. However, there the sectioning is realized using a standard microscopes, an incoherent light source and without the need for a scanning mechanism. For SI microscopy, a grid is imaged into the specimen to produce a one-dimensional sinusoidal excitation pattern in the focal plane. The resulting sinusoidal fluorescence image, consisting of both in- focus and out-of-focus fluorescence emission, is then normally recorded. Several images are taken, each corresponding to a different grid position equivalent to three different phase shifts of the grating. The grid pattern only appears in the focal plane while it is blurred in the out of focus regions. Hence, it is possible to extract an optical section from the spatially modulated component of the images via a simple calculation.

Based on the SI microscopy technique presented by *Neil et al.* in 2005 [27] as well as their earlier work on indirect wavefront sensing using a conventional microscope [13] in 2007 (described in the previous section) *Debarre et al.* combined both techniques in 2008 and proposed an AO scheme for use in SI microscopy [14].

They again present a sensorless wavefront detection scheme, which is shown in Fig. 7. The method to

obtain the aberration correction is similar to the one presented and explained in the previous section. The authors derive an inner product from a mathematical model of the imaging process, followed by an orthogonalization process applied to a set of Zernike polynomials. Based on that, a general method providing an optimal aberration expansion for the chosen optimization metric is presented. This process yields information about the effects of different aberration modes in of the SI microscope. *Debarre et al.* show that the image quality mainly depends on the imaging efficiency spatial frequency of the illumination pattern. This imaging efficiency is affected much more by some aberration modes (called grid modes) than by others (called non-grid modes) . Grid modes have a significant influence on the intensity of the sectioned image, whereas non-grid modes have comparatively little effect. The non-grid modes do however affect the resolution.

The results of the implemented AO scheme is shown in Fig. 8 for aberration correction on a fluorescent mouse intestine. The image contrast and sharpness improvement is clearly visible in image 8b compared to the uncorrected image in 8a. As a result of the aberration correction, and as shown in Fig. 8c, the contrast of small sample features (blue arrows) is better defined after (red solid line) rather than before (black dotted line) correction.

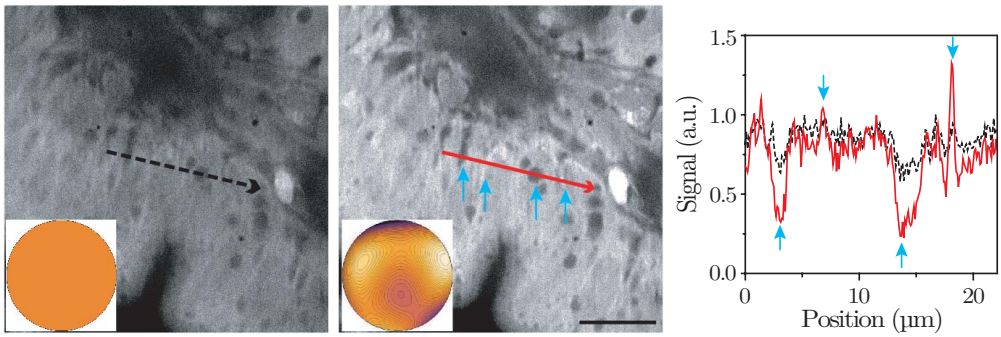

(a) Uncorrected. (b) Corrected. (c) Line Scan.

Figure 8: Aberration correction in structured illumination microscopy. A fluorescent mouse intestine sample was imaged (a) without (b) with aberration correction with inserts showing the phase induced by the deformable mirror. (c) Profile along the lines drawn on the images, both profiles normalized so that their mean value is identical. As a result of the resolution improvement, the contrast of small sample features (blue arrows) is better defined after (red solid line) rather than before (black dotted line) correction. The imaging depth was approximately 10 µm, sacle bar size 10 µm. Image after [14] .

The authors also explain an additional benefit of aberration correction for structured illumination microscopy. That the adaptive element can also be used to improve the rejection of the out-of-focus fluorescence. When imaging thick specimen, noise fluctuations in the fluorescence signal between the three successive widefield images obtained for the maximization process result in a large out-of-focus background in the calculated sectioned images. Since this background arises from fluorescence generated outside the focal plane, it is not sensitive to the presence of aberrations. By applying large aberrations in a number of grid modes, the grid pattern is suppressed and only the out-of-focus noise can be measured. By subtracting this aberrated image from the original sectioned image, the fluorescent background can be efficiently removed, leading to greatly improved contrast of the in-focus structures.

The aberrations can also change significantly with depth and hence using the same correction for different depths can result in a degradation of the image quality. The correction can however be adapted for different imaging depths in the sample. This permits improvement of the image quality throughout an axially extended sample. It is furthermore possible to determined the appropriate modes once and use the same scheme for any specimen, as the scheme is mostly independent of the object structure. Alternatively, if one wants to correct for local variations in aberrations the image could be formed from several sub-images for which independent aberration correction would be performed.

In conclusion, the authors present a sophisticated, easy to implement and highly versatile AOM scheme which allows for aberration correction induced by the optical system, the specimen or the focus

depth. While the presented scheme uses a widefield microscope, *Debarre et al.* are also optimistic that similar AO methods based on indirect, image based aberration detection can be applied to point-scanning methods.

3.2 Point Scanning Microscopes

Just as with the widefield techniques, adaptive optics quickly found its way into point scanning techniques to improve the image and signal quality.

Scanning methods are useful for imaging biological specimens, since they can provide high resolution imaging in three-dimensions. Illumination is usually provided by a laser that is focused into the sample. The light emitted or reflected from the specimen is collected, usually through the same objective lens, and its intensity is measured by a detector. Since this only provides information about the intensity at a single spot, focal point is then scanned through the specimen and point-by-point the image is acquired.

Several other point scanning microscope modalities have been introduced, including Two-Photon Excitation Fuorescence (TPEF) microscopy, second harmonic generation (SHG) and third harmonic generation (THG) microscopy, and coherent anti-Stokes Raman (CARS) microscopy.

- using a fluorescence microscope, the smaller FWHM, provided by the optimized DMM, will increase the excitation intensity leading to a higher fluorescent signal for the same laser beam input power

[21, 29] -> Both the second- and third-harmonic intensity signals are used as the optimization metric - Aberration correction is performed to compensate both system- and specimen-induced aberrations by using an efficient optimization routine based upon Zernike polynomial modes - images of live mouse embryos show an improved signal level and resolution. - The peak intensity increased by almost 50 % and the FWHM decreased by 14 % to 1.22 µm compared with a value of 1.15 µm for an unaberrated system

[41] - signal improvement 3x for samples at a depth of 700 µm and 6x for muscle tissue at a depth of 260 µm - completely random optimization, approach is well suited to CARS microscopy, since photobleaching does not occur - optimization algorithm typically converged after 3000 mirror shapes, mirror speed up to 1kHz this can be pretty fast

[19] (2012) - STED principle [20] (1994) - STED phase mask as well as aberration correction realized using the SLM - aberration correction in both depletion beam (better resolution) and in the excitation beam path (better signal and less noise) - due to depletion image brightness as metric not good, introduced a new metric that seeks to optimize both image brightness and image sharpness in a combined approach, - imaging through a #1.5 coverglass (0.15 mm thicknes) and 55 µm glycerol, Comparing the axial profiles of the STED and AO STED reveals a $\tilde{5}$-fold increase in the peak signal as well as a $\tilde{3}$.2-fold improvement in resolution

-

3.2.1 Confocal Microscopes

The confocal microscopy can be operated in reflection or fluorescence mode. Both are a dual pass system, which means that either the illumination path and the emission path have to be corrected in an AO confocal microscope.

The first attempt to apply AO in confocal microscopy was done by *Martin J. Booth et al.* [11]. They implemented indirect wavefront sensing to a confocal fluorescence microscope in a closed-loop way. Aberration measurement and correction was done sequentially. First a preset positive bias aberration was introduced by a deformable membrane mirror. An image scan was taken and all of its pixel values were summed and averaged to give the value of W_1. Then, it was added to the system the equivalent negative bias aberration, obtaining W_2. They had shown before that the value of the difference signal, W = W_1-W_2, is approximately proportional to the amount of the Zernike mode Zi present in the sample. They applied this procedure for several different Zernike modes, updating the mirror shape each time. A simple representation of the experimental set-up is shown in Fig. 9.

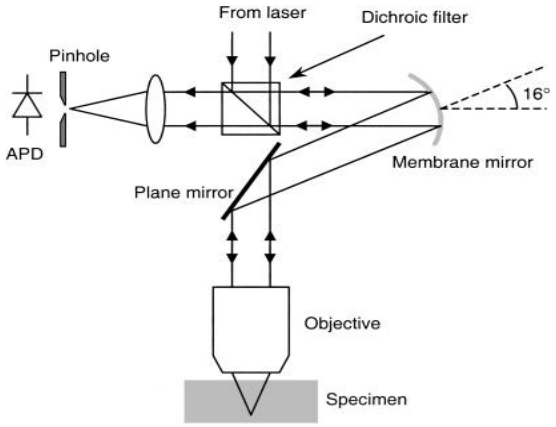

Figure 9: The illumination beam was passed through a beam expander and reflected by the membrane mirror such that the angle between the incident and reflected beams was 16°. Then it passed into the objective lens focusing the light into the specimen. Fluorescence light from the specimen was collected by the same objective. In this configuration, the membrane mirror can compensate for aberrations introduced into both the illumination and emission optical paths.

With this sequential method for correcting aberrations they achieve an axial PSF shorter by a factor of 1.8, using two cycles of this modal wavefront sensor applied to low order aberration modes. Obviously, the degree of correction required and the profit of this method depend upon the nature of each individual specimen.

Another different way to apply AO in confocal microscopy was done by *Xiaodong Tao et al* [36]. They used a direct wavefront sensor in a fluorescence confocal microscope. Particularly, they implemented a Shack-Hartmann sensor with fluorescent micro-spheres (1 μm diameter) embedded in the sample as a point source reference beacons. Their set-up was designed to operate in a close-loop. The corrector device was a deformable mirror. A separate laser channel was added to excite the microsphere, which shared the same light path with the imaging channel. The results showed a 4.3x improvement in the Strehl ratio and a 240 % improvement in the signal intensity for fixed mouse tissues at depths of up to 100 μm. Although the effects of these microspheres in the live tissue have to be further investigated, this direct method enabled a shorter exposure time during sensing and a higher speed of imaging, which showed its potential ability for live in vivo imaging.

3.2.2 Two-Photon Fluorescence Microscopy

Its intrinsic optical sectioning, larger penetration depth, reduced photo damage as well as other advantages allowed nonlinear microscopy in general, and Two-Photon Fluorescence Microscopy (TPFM) in particular, to become a very important tool in biological imaging since its first presentation by *Denk et al.* in 1990 [16]. As with most AO microscopy techniques, both a direct and indirect wavefront sensing scheme can be deployed for the use with TPFM. Indirect sensing was already explained (section 2.2) and presented (section 3.1 in detail. *Marsh et al.* present the first and fairly simple indirect sensing approach, correcting only for depth induced aberrations as early as 2003 [26]. Again, based on their earlier works ([13, 14]), *Débarre et al.* present another highly sophisticated application of their image based wavefront sensing scheme in 2009 [15]. Since both *Marsh* and *Débarre* essentially use the standard TPFM setup and the image optimization is very similar to the one presented earlier, we will not describe these methods here again. *Rueckel et al.* present a wavefront correction method using coherence-gated wavefront sensing [34] which also beyond the scope of this report. This section will therefor describe direct wavefront sensing based on the work presented by *Aviles-Espinosa et al.* in 2011 [2].

For two-photon fluorescence microscopy, it is not essential to correct for sample or system induced

aberrations on the collected beam. Since it is a point scanning technique, all the light emitted in the focus region is collected and only the relative intensity difference is important for the generation of the image (see [28] for a detailed review on TPFM). To achieve the highest possible resolution, especially when imaging deep in a tissue, it is however very important to correct aberrations of the excitation beam. This will not only result in a better, i.e. smaller focus spot, but will also highly increase the efficiency of the nonlinear process. As described in earlier sections, a indirect wavefront sensing is usually applied for microscopic applications. While indirect sensing has several advantages over direct sensing (see sec. 2.2), they have one important drawback that can ultimately not be overcome. They all depend on an iterative optimization procedure to estimate and correct for the aberrations. While random optimization requires many iterations (in some cases up to 3000 iterations per mirror actuator [41]) other methods base the iterations on complicated models and are able to achieve indirect sensing with as little as $2N + 1$ iterations (where N is the number of corrected aberration modes) [13, 14, 15]. However, even these methods require the sample to be exposed and imaged multiple times. To correct 11 aberrations modes (as done in [15]), one needs 23 exposure to acquire an aberration corrected image. While this is suitable for some systems such as CARS where photobleaching is not an issue, it often limits the feasibility of AO in florescence imaging. Being aware of these limitations, *Aviles-Espinosa et al.* therefore developed a direct sensing scheme.

As described in section 2.1, to be able to use a wavefront sensor, one needs a point like reference source which is then used to detect the aberration. This point like source, called "nonlinear guide star" "(NL-GS) by the authors[1], can be artificially created and imbedded in the sample, as done for standard fluorescence microscopy [3]. This however can cause damage to the sample or might influence the behavior of living samples, limiting its potential for in vivo imaging. *Aviles-Espinosa et al.* realized that two-photon excited fluorescence naturally produces a small confined volume which can be used as the guide-star. The setup presented by the authors is shown in Fig. 10. The setup shown is basically an inverted microscope, modified to be used as laser scanning TPFM (see paper for detailed component description and working principle. A mode locked Ti:sapphire laser (λ = 810 nm & 860 nm, pulse duration = 100 fs, repetition rate = 80 MHz, average powers in sample plane = 1.5 mW to 5.6 mW) is used as the excitation beam. The wavefront sensing is performed using a Shack-Hartmann WaveFront Sensor (SH WFS), located at one of the output ports of the microscope. The aberration correction is realized with an electromagnetic Deformable Mirror (DM).

Before the authors started their experiments on biological samples, they first showed that the guide star is reproducible, reliable and independent from the excitation beam aberrations. They continued to verify that the NL-GS behaves as point source as well as proving that aberrations are similar in the complete Field Of View (FOV). Since all these requirements were met, it was show that aberrations in the imaged area can be effectively corrected using only one NL-GS. The authors then continued to calibrate their system, eliminating the passive aberrations of the microscope system coming from the optics for excitation beam as well as the beam path from the objective pupil to the output ports of the microscope. These so called coupling aberrations only need to be corrected once for a given microscopic setup. They were measured and taken into account as a reference for all the subsequent wavefront measurements. The second correction step was to measure the so called focusing aberrations caused by the focusing part of the system. This step was performed every time prior to the actual image acquisition to account for the specific measurement (i.e. the objective, the refractive index matching oil, the cover slip and the sample).

The authors then investigated the performance of their AOM system using both Caenorhabditis elegans and mouse brain samples. -For small aberrations and weak scattering only a modest improvement in signal intensity was shown. At an imaging depth of 25 µm, the measured signal enhancement was 1.75x by correcting the coupling aberrations, and 3.61x when focusing aberrations were corrected as well. Similar values were obtained imaging deeper into the tissue. Caenorhabditis elegans tissue scatterers only weakly and hence spherical aberration is the main aberration for imaging deep into the

[1]The term "guide start" is used in reference to astronomy. There a star or an laser spot projected in the sky is used as the reference and called guide star.

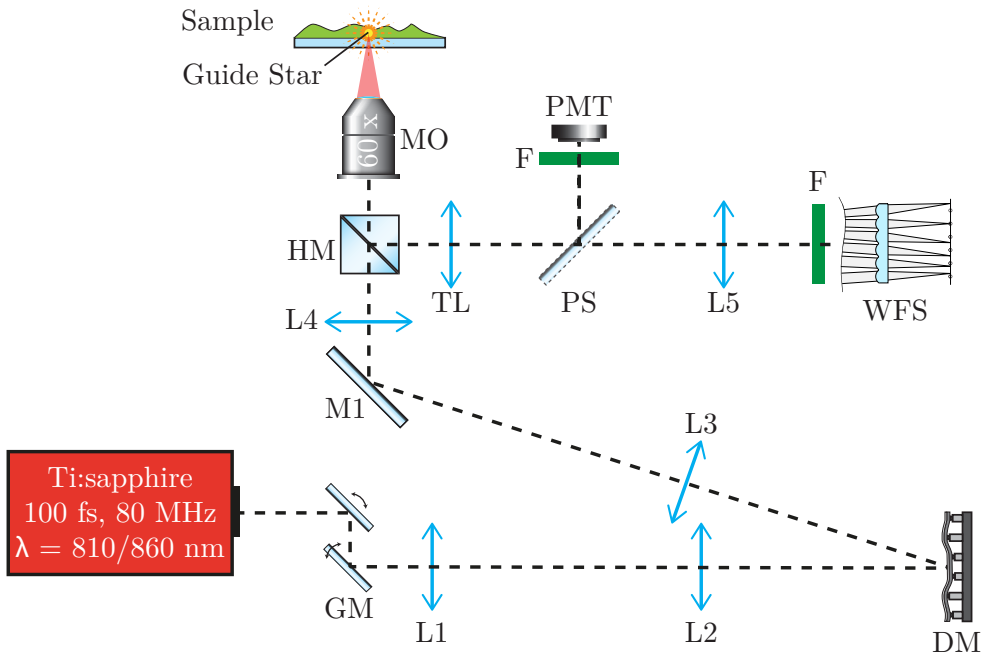

Figure 10: Experimental setup for aberration corrected two-photon fluorescence microscopy as proposed by *Aviles-Espinosa et al.*. GM - galvanometric mirrors, L1-L5 - lenses, DM - deformable mirror, M1 - mirror, HM - filter and beamsplitter, MO - microscope objective, TL - microscope tube lens, F - band pass filters, PMT - photo multiplier tube, WFS - Shack-Hartmann wavefront sensor. The microscope output port is manually selected either for the PMT or for the WF sensor using PS. See [2] for the original image as well as a detailed description of the working principle.

tissue. Since these should be easily corrected using the presented scheme, the authors were surprised by these relatively small improvements if the signal quality. By using an additional agar pad to simulate moderate scattering as well as imaging deeper into the tissue, the authors investigated the correction efficiency further. Deep in the sample (127 µm) where large sample induced aberrations are prominent, improvements of the signal intensity by a factor of 22.59 were possible, as shown in Fig. 11. It is noteworthy, that the aberration correction increases the signals local maxima while the local minima remain unaltered.

Finally, the authors investigate the AO system performance using strongly scattering mouse brain tissue. They show that a correction is still possible, but it is less efficient than for moderately scattering samples. It is furthermore possible to record aberration corrected images with a single exposure, no need for complex optimization algorithms and without further sample preparation (i.e. no fluorescent beads need to be inserted). This minimize photobleaching effects, photo-toxicity and limits negative effects to the living sample. Since no model is needed to correct the aberrations, the method is robust and can be applied to fixed and in vivo biological samples. An overall intensity improvement of more than one order of magnitude was shown is some cases. In conclusion, the authors present and flexible and versatile appication of adaptive optics in microscopy which can be used in wide range biological imaging applications where a high resolution is required.

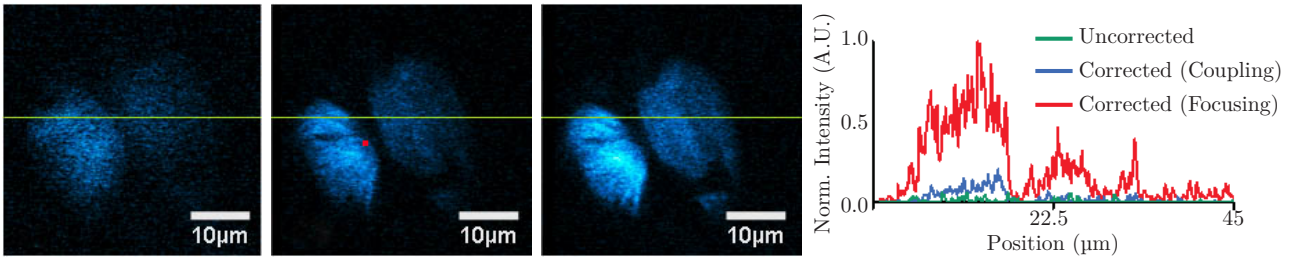

(a) Uncorrected. (b) Coupling cor. (c) Focusing cor. (d) Line Scan.

Figure 11: In vivo C. elegans sample imaged at 127 µm depth. (a) shows the uncorrected image of a worm section, (b) displays the same section with coupling correction applied and (c) shows the section when both coupling and focusing aberrations are corrected. (d) shows the intensity profile along the green line in the images for all three correction cases. The correction of coupling aberrations improves the signal intensity by a factor of only 1.94 whereas the correction of both coupling and focusing aberrations results in a very good improvement of 22.59. Image after [2].

4 Conclusion & Future Prospects

Adaptive Optics have been applied in many fields for more than fifteen years, however, in biological imaging it is relatively new to use AO systems. It still needs more research before AO can become a regular component of laboratory microscopes, the particular characteristics of microscopes make AO specially difficult to implement it.

The first think it is important to remark in AO applied to microscopy is that correcting aberrations does not give us high resolution or superesolution by itself. It gives us an improvement in axial and lateral resolution as well as an increase in signal intensity, in other words, AO extend the capabilities of high-resolution or superesolution techniques. Moreover, the advantages of correcting aberrations will always depend on the specimen under study and the microscopy technique used. One of the most critical issues in AO applied to microscopy is the accuracy in the sensing process, that is, how we obtain the aberration information from the sample. It seems to be that indirect sensing is the first option in almost all the experiments for AO microscopes, that is because it is more suitable and easy to implement in microscopy since only requires a deformable mirror, although it is less faster than direct sensing. Regarding the choice of a direct or indirect methods, we can say in general terms that, if we care more about the speed of measurement and photobleaching is a problem, direct sensing is likely to be the right choice. But, if care more about the signal intensity and photobleaching is not a problem in our experiment, indirect sensing might be the right choice. Although at the end, the right choice will be determined by the microscopy technique as well. Despite all this, further improvements in the sensing process will extend the microscope's ability to image samples with large and more complex aberrations.

Another important aspect in AO for microscopy is that aberrations don't change quickly when we just consider a small region of a biological sample. In this sense, the time response of the current corrector devices is enough. However, as long as we want to scan different parts of the sample, aberrations can change significantly because the refractive index of the specimen varies throughout its volume. Thus, we need to implement in a microscope a faster corrector device or multiple corrector devices in the same AO system. This last solution still needs to be further investigated in microscopy. Also, to our knowledge, AO applications in techniques such as STORM/PALM need still to be experimented. Finally, another future prospect that is essential for live imaging is that further improvements in both, the speed of the sensing process and the time response of the corrector devices, will extend the ability to correct aberrations in real time and with less exposure of the specimens during the measurement.

References

[1] O. Albert, L. Sherman, G. Mourou, T. B. Norris, and G. Vdovin. Smart microscope: an adaptive optics learning system for aberration correction in multiphoton confocal microscopy. *Opt. Lett.*, 25(1):52–54, Jan 2000.

[2] Rodrigo Aviles-Espinosa, Jordi Andilla, Rafael Porcar-Guezenec, Omar E. Olarte, Marta Nieto, Xavier Levecq, David Artigas, and Pablo Loza-Alvarez. Measurement and correction of in vivo sample aberrations employing a nonlinear guide-star in two-photon excited fluorescence microscopy. *Biomed. Opt. Express*, 2(11):3135–3149, Nov 2011.

[3] Oscar Azucena, Justin Crest, Jian Cao, William Sullivan, Peter Kner, Donald Gavel, Daren Dillon, Scot Olivier, and Joel Kubby. Wavefront aberration measurements and corrections through thick tissue using fluorescent microsphere reference beacons. *Opt. Express*, 18(16):17521–17532, Aug 2010.

[4] Oscar Azucena, Justin Crest, Shaila Kotadia, William Sullivan, Xiaodong Tao, Marc Reinig, Donald Gavel, Scot Olivier, and Joel Kubby. Adaptive optics wide-field microscopy using direct wavefront sensing. *Opt. Lett.*, 36(6):825–827, Mar 2011.

[5] H. W. Babcock. The possibility of compensating astronomical seeing. *Pub. Astron. Soc. Pacific*, 65, Oct 1953.

[6] Jörg Bewersdorf, Rainer Pick, and Stefan W. Hell. Multifocal multiphoton microscopy. *Opt. Lett.*, 23(9):655–657, 5 1998.

[7] Martin Booth. Wave front sensor-less adaptive optics: a model-based approach using sphere packings. *Opt. Express*, 14(4):1339–1352, Feb 2006.

[8] Martin J. Booth. Wavefront sensorless adaptive optics for large aberrations. *Opt. Lett.*, 32(1):5–7, Jan 2007.

[9] Martin J. Booth. *Adaptive Optics in Microscopy*, pages 295–322. Wiley-VCH Verlag GmbH & Co. KGaA, 2011.

[10] Martin J. Booth, Delphine Débarre, and Alexander Jesacher. Adaptive optics for biomedical microscopy. *Opt. Photon. News*, 23(1):22–29, 1 2012.

[11] Martin J. Booth, Mark A. A. Neil, Rimas Juškaitis, and Tony Wilson. Adaptive aberration correction in a confocal microscope. *Proceedings of the National Academy of Sciences*, 99(9):5788–5792, 4 2002.

[12] Simao Coelho, Simon Poland, Nikola Krstajic, David Li, James Monypenny, Richard Walker, David Tyndall, Tony Ng, Robert Henderson, and Simon Ameer-Beg. Multifocal multiphoton microscopy with adaptive optical correction. *Proc. SPIE*, 8588:858817–858817–12, 2013.

[13] Delphine Debarre, Martin J. Booth, and Tony Wilson. Image based adaptive optics through optimisation of low spatial frequencies. *Opt. Express*, 15(13):8176–8190, 6 2007.

[14] Delphine Débarre, Edward J. Botcherby, Martin J. Booth, and Tony Wilson. Adaptive optics for structured illumination microscopy. *Opt. Express*, 16(13):9290–9305, 6 2008.

[15] Delphine Débarre, Edward J. Botcherby, Tomoko Watanabe, Shankar Srinivas, Martin J. Booth, and Tony Wilson. Image-based adaptive optics for two-photon microscopy. *Opt. Lett.*, 34(16):2495–2497, 8 2009.

[16] W Denk, JH Strickler, and WW Webb. Two-photon laser scanning fluorescence microscopy. *Science*, 248(4951):73–76, 1990.

[17] J. R. Fienup and J. J. Miller. Aberration correction by maximizing generalized sharpness metrics. *J. Opt. Soc. Am. A*, 20(4):609–620, Apr 2003.

[18] Frédéric Gonté, Alain Courteville, and René Dändliker. Optimization of single-mode fiber coupling efficiency with an adaptive membrane mirror. *Optical Engineering*, 41(5):1073–1076, 2002.

[19] Travis J. Gould, Daniel Burke, Joerg Bewersdorf, and Martin J. Booth. Adaptive optics enables 3d sted microscopy in aberrating specimens. *Opt. Express*, 20(19):20998–21009, 9 2012.

[20] Stefan W. Hell and Jan Wichmann. Breaking the diffraction resolution limit by stimulated emission: stimulated-emission-depletion fluorescence microscopy. *Opt. Lett.*, 19(11):780–782, Jun 1994.

[21] Alexander Jesacher, Anisha Thayil, Kate Grieve, Delphine Débarre, Tomoko Watanabe, Tony Wilson, Shankar Srinivas, and Martin Booth. Adaptive harmonic generation microscopy of mammalian embryos. *Opt. Lett.*, 34(20):3154–3156, 10 2009.

[22] P. KNER, J.W. SEDAT, D.A. AGARD, and Z. KAM. High-resolution wide-field microscopy with adaptive optics for spherical aberration correction and motionless focusing. *Journal of Microscopy*, 237(2):136–147, 2010.

[23] W. Lukosz. Der einfluß der aberrationen auf die optische Übertragungsfunktion bei kleinen ortsfrequenzen. *Optica Acta: International Journal of Optics*, 10(1):1–19, 1963.

[24] Virendra N. Mahajan. *Optical Imaging and Aberrations, Part II. Wave Diffraction Optics (SPIE Press Monograph Vol. PM209)*. SPIE Press, 2 edition, 8 2011.

[25] Daniel Malacara, editor. *Optical Shop Testing (Wiley Series in Pure and Applied Optics)*. Wiley-Interscience, 3 edition, 7 2007.

[26] P. Marsh, D. Burns, and J. Girkin. Practical implementation of adaptive optics in multiphoton microscopy. *Opt. Express*, 11(10):1123–1130, 5 2003.

[27] M. A. A. Neil, R. Juskaitis, and T. Wilson. Method of obtaining optical sectioning by using structured light in a conventional microscope. *Opt. Lett.*, 22(24):1905–1907, Dec 1997.

[28] Martin Oheim, Darren J. Michael, Matthias Geisbauer, Dorte Madsen, and Robert H. Chow. Principles of two-photon excitation fluorescence microscopy and other nonlinear imaging approaches. *Advanced Drug Delivery Reviews*, 58(7):788 – 808, 2006.

[29] Nicolas Olivier, Delphine Débarre, and Emmanuel Beaurepaire. Dynamic aberration correction for multiharmonic microscopy. *Opt. Lett.*, 34(20):3145–3147, 10 2009.

[30] B. C. Platt and R. Shack. History and principles of shack-hartmann wavefront sensing. *Journal of refractive surgery*, 17(5), October 2001.

[31] Jason Porter, Hope Queener, Julianna Lin, Karen Thorn, and Abdul A. S. Awwal. *Adaptive Optics for Vision Science: Principles, Practices, Design and Applications (Wiley Series in Microwave and Optical Engineering)*. Wiley-Interscience, 1 edition, 7 2006.

[32] William H. Press, Saul A. Teukolsky, William T. Vetterling, and Brian P. Flannery. *Numerical Recipes 3rd Edition: The Art of Scientific Computing*. Cambridge University Press, 3 edition, 9 2007.

[33] Francçois Roddier. Curvature sensing and compensation: a new concept in adaptive optics. *Appl. Opt.*, 27(7):1223–1225, Apr 1988.

[34] Markus Rueckel, Julia A. Mack-Bucher, and Winfried Denk. Adaptive wavefront correction in two-photon microscopy using coherence-gated wavefront sensing. *Proceedings of the National Academy of Sciences*, 103(46):17137–17142, 2006.

[35] M. Schwertner, M. Booth, and T. Wilson. Characterizing specimen induced aberrations for high na adaptive optical microscopy. *Opt. Express*, 12(26):6540–6552, 12 2004.

[36] Xiaodong Tao, Bautista Fernandez, Oscar Azucena, Min Fu, Denise Garcia, Yi Zuo, Diana C. Chen, and Joel Kubby. Adaptive optics confocal microscopy using direct wavefront sensing. *Opt. Lett.*, 36(7):1062–1064, Apr 2011.

[37] Larry N. Thibos. Principles of hartmann-shack aberrometry. In *Vision Science and its Applications*. Optical Society of America, 2000.

[38] Robert Tyson. *Adaptive Optics Engineering Handbook (Optical Science and Engineering)*. CRC Press, 1 edition, 11 1999.

[39] Paolo Villoresi, Stefano Bonora, Michele Pascolini, Luca Poletto, Giuseppe Tondello, Caterina Vozzi, Mauro Nisoli, Giuseppe Sansone, Salvatore Stagira, and Sandro De Silvestri. Optimization of high-order harmonic generation by adaptive control of a sub-10-fs pulse wave front. *Opt. Lett.*, 29(2):207–209, Jan 2004.

[40] Ingolf Weingaertner and Michael Schulz. Interferometric methods for the measurement of wavefront aberrations. *Proc. SPIE*, 1781:266–279, 1993.

[41] A. J. Wright, S. P. Poland, J. M. Girkin, C. W. Freudiger, C. L. Evans, and X. S. Xie. Adaptive optics for enhanced signal in cars microscopy. *Opt. Express*, 15(26):18209–18219, 12 2007.

[42] F. Zernike. Beugungstheorie des schneidenver-fahrens und seiner verbesserten form, der phasenkontrastmethode. *Physica*, 1(7–12):689 – 704, 1934.